

Chapter 13

Ultrafast Inner-Shell Electron Excitation with High Energy Recollision Electron Driven by Mid-infrared Laser



Z. Zeng, Y. Deng, Y. Zheng, G. Marcus and R. Li

Abstract As one of the most important physical processes of strong-field laser-matter interaction, laser-driven electron-ion recollision is the fundamental process. As we have known, the well-known three-step model of HHG predicts that the cutoff law obeys $E_{\text{cutoff}} = I_p + 3.17U_p$, implying that the maximum kinetic energy of returning electron can be greatly extended by increasing the driving wavelength. With the long wavelength mid-infrared laser pulse, it is easy for the ponderomotive energy of the returning electron to be very large to excite the deep inner-shell electron, which may be used to investigate the ultrafast inner-shell electron dynamics.

13.1 Introduction

High-order harmonics generated by the interaction of extremely intense laser field with noble and simple polyatomic gases have been extensively studied and utilized to produce an intense coherent XUV or X-ray light source [1–3] to synthesize isolated attosecond pulses (IAPs) or attosecond pulse trains (APTs) by synchronizing harmonics near the cutoff region [4] to probe ultrafast dynamics of tunneling ionization (TI) and rescattering of electron wavepacket (EWP) of molecules and atoms with attosecond precision [5–8]. The process, which is frequently referred to as high-order harmonic generation (HHG), has been intuitively clarified by Corkum's three-step model [9]. The three-step model of HHG predicts that the cutoff law obeys $E_{\text{cutoff}} = I_p + 3.17U_p$ (I_p is the ionization potential. $U_p \propto I\lambda^2$ is the ponderomotive energy), implying that the maximum kinetic energy of returning electron can

Z. Zeng (✉) · Y. Zheng · R. Li

State Key Laboratory of High Field Laser Physics, Shanghai Institute of Optics and Fine Mechanics, Chinese Academy of Sciences, Shanghai 201800, China
e-mail: zhinan_zeng@mail.siom.ac.cn

Y. Deng

SwissFEL, Paul Scherrer Institut (PSI), 5232 Villigen, Switzerland

G. Marcus

Department of Applied Physics, Benin School of Engineering and Computer Science, Hebrew University of Jerusalem, 91904 Jerusalem, Israel

© Springer Nature Switzerland AG 2020

M. Kozlová and J. Nejdil (eds.), *X-Ray Lasers 2018*, Springer Proceedings in Physics 241, https://doi.org/10.1007/978-3-030-35453-4_13

be greatly extended by increasing the driving wavelength. With the long wavelength mid-infrared laser pulse, it is easy for the kinetic energy of the returning electron to be very large to excite the deep inner-shell electron.

The excitations of electrons from deeper shells are usually accompanied by multi-electron dynamics such as double excitation, the Auger decay, Cooper minima, and the giant resonance, which cannot be explained by the single active electron approximation. Such excitations are unstable and usually decay on a time scale ranging from few femtoseconds to a few attoseconds [10, 11]. The decay may take place in a single step, but more often occurs as a cascade of radiative and nonradiative channels. Spectroscopic data may give some general information about the nature of such dynamics but often fail to follow the exact details, for example, the line widths of the cascade Auger decays reveal the total decay rate but not the order of decaying channels and their individual decay rate. To really follow such dynamics, one resorts to a time-domain spectroscopy [11–13], in which a first “pulse” initiates the process and a second “pulse” probes it. Since the relevant time scale for such dynamics spans from attoseconds to femtoseconds and the relevant energy scale spans from 10^2 to 10^5 eV, X-ray attosecond bursts may be the choice to serve as the pump and the probe events. However, with the low photon flux of current soft X-ray attosecond sources ($\hbar\omega > 300$ eV) and the low absorption cross sections in this spectral range, it is currently impossible to both pump and probe these processes with attosecond X-ray pulses. To probe processes involving valence electrons, an ultrashort infrared pulse is often used to initiate the process, and a well-synchronized extreme ultraviolet (XUV) attosecond pulse probes it [14]. It is difficult to extend this scheme to excite inner-shell processes because of the large energy difference between inner-shell energies and the infrared photon energy. Excitation of inner-shell dynamics by laser-induced electron recollision might be the solution. Here, we show direct evidence for such excitations, as opposed to previous indirect evidence [15, 16]. Such an excitation process occurs in a sub-femtosecond time scale, and thus, provides the necessary “pump” step and might become the key for future “pump-probe” studies of inner-shell dynamics.

13.2 Experiments and Results

In our experiment, we focus a 12 fs, 1 mJ infrared radiation source ($\lambda_0 = 1.8 \mu\text{m}$) on a pulsed gas jet and observed the soft X-ray radiation from the interaction region. Because of the quadratic scaling of the ponderomotive energy, such infrared sources have already demonstrated the extension of HHG spectra toward the soft X-ray range ($\hbar\omega > 1$ keV) [15]. The infrared radiation source we have used here is based on an optical parametric amplifier, described in detail elsewhere [17]. The soft X-ray radiation that is coming from the excited atoms is a measure of the amount of excitation, but in order to separate it from the accompanying HHG radiation, we observed the soft X-ray radiation at a right angle to the infrared propagation direction. The infrared beam was focused on the gas target placed inside a vacuum chamber

by a $f = 300$ mm CaF_2 lens to a spot size of about $65 \mu\text{m}$ FWHM, which results in a peak intensity of about 3×10^{15} W/cm^2 . The corresponding ponderomotive energy is about 900 eV, enough to excite the K shell of neon and the L shell of krypton. For the gas target we used jets of neon and krypton from a pulsed nozzle (series 9 Parker nozzle, orifice diameter of $350 \mu\text{m}$ and backing pressures ranging from 1 to 10 bar), the pulsed nozzle was operated at 20 Hz to keep the pressure inside the vacuum chamber below 10^{-3} mbar. Soft X-ray spectra from the krypton and the neon atom were recorded by a silicon drift detector (Amptek XR-100SDD) with a $12.5 \mu\text{m}$ beryllium window, positioned 350 mm away from the interaction region. During the experiment, we firstly scanned the focus position along the gas propagation direction to find the best X-ray yield. We obtained the best X-ray yield when we placed the beam focus just next to the nozzle exit; all of the results were taken at this position.

Figure 13.1 shows the soft X-ray spectra coming from Ne and Kr targets. The spectrum shows the characteristic K-shell line from Ne and L-shell line from Kr, on top of a wider continuum. The continuum radiation from Kr extends up to ~ 2800 eV which is in good agreement with the abovementioned formula for the maximum possible kinetic energy of the recolliding electron: $K_{\text{max}} = 3.17U_p = 2.96 \times 10^{-13} I_0 \lambda^2$ (K is in eV, I_0 is in W/cm^2 and λ is in μm). We speculate that the origin of this continuum is either coming from the recombination radiation or from the bremsstrahlung radiation. The sharp cutoff at the lower energy end is due to absorption in the beryllium window.

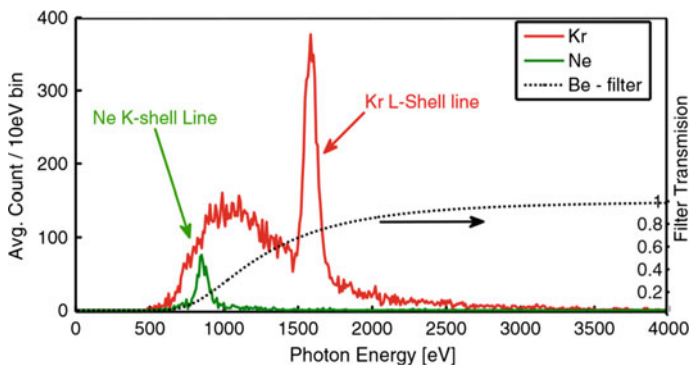


Fig. 13.1 The fluorescence spectra from the excited Ne (green line) and Kr (red line) atoms. The signal from the Ne is mainly from the K-shell transition with a weak continuum that stretches up to ≈ 1600 eV. In the Kr spectrum there is a sharp line, belonging to the L-shell transition, on top of a pronounced continuum. (The resolution of the SDD detector is not high enough to resolve the $L\alpha$, $L\beta$ splitting.) The above Ne spectrum and the Kr spectrum were taken at different conditions. The Kr spectrum was taken during an integration time of 85 min and backing pressure of 4 bar; the Ne spectrum was taken during an integration time of 170 min and backing pressure of 10 bar. Also given in this figure is the transmission curve of the $12.5 \mu\text{m}$ thick beryllium window (black dotted line). Taking into account the repetition rate, integration time, and distance of the detector from the target, we estimate the total number of photons/pulse going into 4π as 10000 photons from Kr and 300 photons from Ne. The beryllium absorption is not included in the calculation

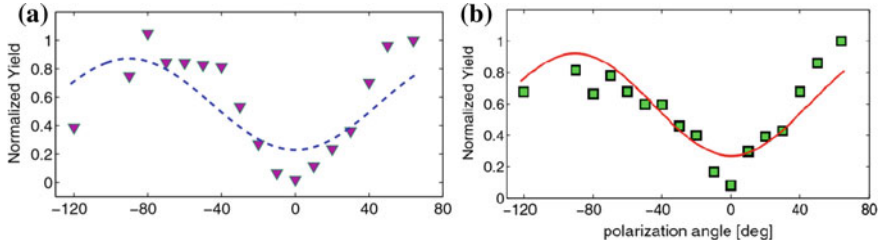


Fig. 13.2 The krypton L-shell fluorescence yield (a) and the continuum yield (b) as a function of the angle between polarization direction and detector direction. We fit the fluorescence yield to the $I(\theta)/I(\pi/2) = 1 - P\cos^2\theta$ formula (blue broken line, $P = 0.716$) and the continuum with the modified Sommerfeld formula which is given above (red solid line, $P = 0.78$). Measuring conditions: backing pressure of 4 bars, 5 min integration time for each point

The goal of this study is to show that the core-hole excitations we have observed are indeed coming from the recollision process and not from mere heating of the plasma. As a first step toward this goal, we followed the reasoning of [18] and tested the fluorescence and the continuum directionality. For that purpose, we used a $\lambda/2$ waveplate to rotate the polarization direction with respect to the position of the detector and measured both the X-ray fluorescence and the continuum yield as a function of that direction. We observed a minimum in both of them when the polarized field pointed toward the detector and a maximum when it was approximately perpendicular to that direction (see Fig. 13.2).

With the pulse duration of our IR source (only 2 cycle) and the gas densities we worked at 10^{17} – 10^{18} cm^{-3} ; we are not expecting the inverse bremsstrahlung (IB) and ATI heating to play an important role in the observed core-hole excitations. The dipole like radiation pattern (Fig. 13.2) strongly supports the recollision excitation mechanism over the IB and ATI heating processes. As a next step for testing whether we have recollision excitation or not, we checked how the X-ray yield depends on the drive's ellipticity, since the recollision process is highly sensitive to the polarization ellipticity of the drive [19]. According to the most simplified recollision model, in which the electron emerges from the deformed Coulomb barrier with a zero velocity, as the ellipticity gets larger and larger, the electron trajectories are pushed away from the parent ion and never come back to recollide with it. Therefore, it is common practice to check whether a process is coming from the recollision process or not by changing the drive polarization ellipticity. Figure 13.3a shows the x-ray yield from the Kr target as a function of the drive ellipticity.

Indeed, we can see a strong reduction in the X-ray yield as the ellipticity grows. However, as the ellipticity grows, the infrared peak intensity is reduced and leads to a reduced ionization rate which can partially explain the reduction of the photon yield. To check if the reduction in the photon yield is due to the lower ionization yield or due to the deflection of the returning electron, we compare again the results from the linear polarization drive and the circular polarization drive, this time we keep the peak electric field the same (see Fig. 13.3b). This test shows clearly that the main reduction

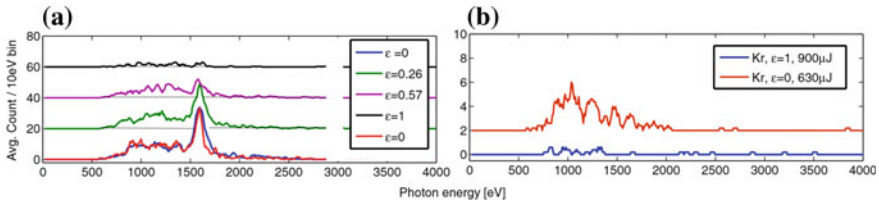


Fig. 13.3 **a** The X-ray radiation yield from the Kr atoms versus the drive ellipticity (backing pressure: 4 bar, integration time: 20 min per spectrum, laser energy 1050 μJ). **b** Comparison of the X-ray yield when using a linearly polarized or circularly polarized infrared drive while keeping the peak electric field the same (backing pressure 4 bar, integration time of 60 min for each spectrum)

in the X-ray yield is a result of the electron deflection by the circular polarization. Nevertheless, the signal does not completely disappear with circular polarization as one would expect from the most simplified recollision induced excitation model. This residual X-ray emission might have a connection to other recently reported findings from other groups. A nonsequential double ionization with circular polarization was reported by a few groups [20–23]. Mizuno et al. observed an extended tail in the spectrum of the photoelectrons from the interaction of a strong circular laser field with Kr atoms, such a tail was believed to be a signature for electron recollision. An explanation for all these findings might be given by an extended recollision model. In this extended model, the initial velocity of the electron just at the emergence time from the tunneled barrier is not necessarily equal to zero but has some distribution, both along the radiation polarization [24] as well as in the transverse direction [25, 26]. Some of these initial velocities allow for recollisions even with circularly polarized radiation [23, 27, 28]. Another option is a “shake-up” process, in which tunnel ionization results in simultaneous excitation of one or more of the remaining electrons [22]. It is also possible that the gas jet is thick enough to allow for fast ATI electrons to collide with atoms within the jet and excite them.

13.3 Conclusion

In conclusion, the dipole like radiation pattern (Fig. 13.2) and the strong dependency of the X-ray emission on the drive ellipticity (Fig. 13.3) are strong evidence supporting the recollision excitation mechanism over the IB and ATI heating processes [29]. Since the recollision excitation process occurs at the sub-femtosecond time scale, it opens the door for time-domain studies of electron dynamics in highly excited states where the recollision event initiates the excitation followed by a synchronized attosecond probe pulse.

References

1. T. Ditmire, E.T. Gumbrell, R.A. Smith, J.W.G. Tisch, D.D. Meyerhofer, M.H.R. Hutchinson, Spatial coherence measurement of soft x-ray radiation produced by high order harmonic generation. *Phys. Rev. Lett.* **77**, 4756–4759 (1996)
2. M. Bellini, C. Lyngå, A. Tozzi, M.B. Gaarde, T.W. Hänsch, A. L’Huillier, C.-G. Wahlström, Temporal coherence of ultrashort high-order harmonic pulses. *Phys. Rev. Lett.* **81**, 297–300 (1998)
3. P. Salières, A. L’Huillier, M. Lewenstein, Coherence control of high-order harmonics. *Phys. Rev. Lett.* **74**, 3776–3779 (1995)
4. Y. Mairesse, A. deBohan, L.J. Frasinski, H. Merdji, L.C. Dinu, P. Monchicourt, P. Breger, M. Kovačev, R. Taïeb, B. Carré, H.G. Muller, P. Agostini, P. Salières, Attosecond synchronization of high-harmonic soft x-rays. *Science* **302**, 1540–1543 (2003)
5. H. Niikura, H.J. Wörner, D.M. Villeneuve, P.B. Corkum, Probing the spatial structure of a molecular attosecond electron wavepacket using shaped recollision trajectories. *Phys. Rev. Lett.* **107**, 093004 (2011)
6. M. Kitzler, M. Lezius, Spatial control of recollision wavepackets with attosecond precision. *Phys. Rev. Lett.* **95**, 253001 (2005)
7. A. Baltuška, T. Udem, M. Uiberacker, M. Hentschel, E. Goulielmakis, C. Gohle, R. Holzwarth, V.S. Yakovlev, A. Scrinzi, T.W. Hänsch, F. Krausz, Attosecond control of electronic processes by intense light fields. *Nature* **421**, 611–615 (2003)
8. D. Shafir, Y. Mairesse, D.M. Villeneuve, P.B. Corkum, N. Dudovich, Atomic wavefunctions probed through strong-field light–matter interaction. *Nat. Phys.* **5**, 412–416 (2009)
9. P.B. Corkum, Plasma perspective on strong field multiphoton ionization. *Phys. Rev. Lett.* **71**, 1994–1997 (1993)
10. M. Drescher, M. Hentschel, R. Kienberger, M. Uiberacker, V. Yakovlev, A. Scrinzi, T. Westerwalbesloh, U. Kleineberg, U. Heinzmann, F. Krausz, *Nature (London)* **419**, 803 (2002)
11. F. Penent, J. Palaudoux, P. Lablanquie, L. Andric, R. Feifel, J.H.D. Eland, *Phys. Rev. Lett.* **95**, 083002 (2005)
12. T. Uphues, M. Schultze, M.F. Kling, M. Uiberacker, S. Hendel, U. Heinzmann, N.M. Kabachnik, M. Drescher, *New J. Phys.* **10**, 025009 (2008)
13. A.J. Verhoef, A.V. Mitrofanov, X.T. Nguyen, M. Krikunova, S. Fritzsche, N.M. Kabachnik, M. Drescher, A. Baltuška, *New J. Phys.* **13**, 113003 (2011)
14. F. Krausz, M. Ivanov, *Rev. Mod. Phys.* **81**, 163 (2009)
15. G. Marcus, W. Helml, X. Gu, Y. Deng, R. Hartmann, T. Kobayashi, L. Strueder, R. Kienberger, F. Krausz, *Phys. Rev. Lett.* **108**, 023201 (2012)
16. A.D. Shiner, B.E. Schmidt, C. Trallero-Herrero, H.J. Wörner, S. Patchkovskii, P.B. Corkum, J.-C. Kieffer, F. Legare, D.M. Villeneuve, *Nat. Phys.* **7**, 464 (2011)
17. C. Zhang, P. Wei, Y. Huang, Y. Leng, Y. Zheng, Z. Zeng, R. Li, Z. Xu, *Opt. Lett.* **34**, 2730 (2009)
18. S. Dobsz, M. Lezius, M. Schmidt, P. Meynadier, M. Perdrix, D. Normand, J.-P. Rozet, D. Vernhet, *Phys. Rev. A* **56**, R2526 (1997)
19. K.S. Budil, P. Salières, M.D. Perry, A. L’Huillier, *Phys. Rev. A* **48**, R3437 (1993)
20. G.D. Gillen, M.A. Walker, L.D. Van Woerkom, *Phys. Rev. A* **64**, 043413 (2001)
21. C. Guo, G.N. Gibson, *Phys. Rev. A* **63**, 040701 (2001)
22. W.A. Bryan et al., *Nat. Phys.* **2**, 379 (2006)
23. F. Mauger, C. Chandre, T. Uzer, *Phys. Rev. Lett.* **105**, 083002 (2010)
24. A.N. Pfeiffer, C. Cirelli, A.S. Landsman, M. Smolarski, D. Dimitrovski, L.B. Madsen, U. Keller, *Phys. Rev. Lett.* **109**, 083002 (2012)
25. M.Y. Ivanov, M. Spanner, O. Smirnova, *J. Mod. Opt.* **52**, 165 (2005)
26. L. Arissian, C. Smeenk, F. Turner, C. Trallero, A.V. Sokolov, D.M. Villeneuve, A. Staudte, P.B. Corkum, *Phys. Rev. Lett.* **105**, 133002 (2010)
27. N.I. Shvetsov-Shilovski, S.P. Goreslavski, S.V. Popruzhenko, W. Becker, *Phys. Rev. A* **77**, 063405 (2008)

28. X. Wang, J.H. Eberly, *New J. Phys.* **12**, 093047 (2010)
29. Yunpei Deng, Zhinan Zeng, Zhengmao Jia, Pavel Komm, Yinhui Zheng, Xiaochun Ge, Ruxin Li, Gilad Marcus, Ultrafast excitation of an inner-shell electron by laser-induced electron recollision. *Phys. Rev. Lett.* **116**, 073901 (2016)